Composition-dependent oxygen vacancy formation in multicomponent wide-band-gap oxides

Altynbek Murat and Julia E. Medvedeva*

Department of Physics, Missouri University of Science and Technology, Rolla, Missouri 65409, USA

(Received 17 April 2012; revised manuscript received 19 July 2012; published 16 August 2012)

The formation and distribution of oxygen vacancy in layered multicomponent $InAMO_4$ oxides with A^{3+} = Al or Ga and M^{2+} = Ca or Zn and in the corresponding binary oxide constituents is investigated using first-principles density functional calculations. Comparing the calculated formation energies of the oxygen defect at six different site locations within the structurally and chemically distinct layers of $InAMO_4$ oxides, we find that the vacancy distribution is significantly affected not only by the strength of the metal-oxygen bonding, but also by the cation's ability to adjust to anisotropic oxygen environment created by the vacancy. In particular, the tendency of Zn, Ga, and Al atoms to form stable structures with low-oxygen coordination results in nearly identical vacancy concentrations in the $InO_{1.5}$ and $GaZnO_{2.5}$ layers in $InGaZnO_4$, and only an order of magnitude lower concentration in the $AlZnO_{2.5}$ layer as compared to the one in the $InO_{1.5}$ layer in $InAlZnO_4$. The presence of two light-metal constituents in the $InAlCaO_4$ along with Ca failure to form a stable fourfold coordination as revealed by its negligible relaxation near the defect, leads to a strong preference of the oxygen vacancy to be in the $InO_{1.5}$ layer. Based on the results obtained, we derive general rules on the role of chemical composition, local coordination, and atomic relaxation in the defect formation and propose an alternative light-metal oxide as a promising constituent of multicomponent functional materials with tunable properties.

DOI: 10.1103/PhysRevB.86.085123 PACS number(s): 71.20.Nr, 72.80.Jc

I. INTRODUCTION

The presence of light main-group metals such as Al, Mg, or Ca in multicomponent transparent conducting and semiconducting oxides[1–27] is highly attractive since these cations help stabilize the multication structure, allow for a broader optical transmission window due to a larger band gap, and also help control the carrier content while preserving the carrier mobility. The little sensitivity of the mobility on the chemical composition can be explained based on the results of the electronic band structure investigations of undoped stoichiometric $InAMO_4$ compounds with A^{3+} = Al or Ga and M^{2+} = Ca or Zn. It was shown[28] that the electronic properties of these layered-structured multicomponent oxides resemble those in the conventional binary transparent conductive oxides (TCOs): both exhibit a dispersed *s*-like conduction band and possess a small (0.3–0.5 m_e), isotropic electron effective mass. Strikingly, it was found that despite the different band gaps of the constituent basis binary oxides (2–4 eV In_2O_3 or ZnO; 5 eV for Ga_2O_3; and 7–9 eV in CaO or Al_2O_3), the states of *all* cations contribute to the bottom of the conduction band of the multicomponent oxide. Such a hybrid conduction band is expected to provide a uniform network for the carrier transport within and across the chemically and structurally distinct layers of the $InAMO_4$ materials.

In this work, we study the electronic properties of oxygen deficient $InGaZnO_4$, $InAlZnO_4$, and $InAlCaO_4$ to determine how the chemical composition affects the formation of the electron donor defects. By comparing the calculated formation energies of the oxygen vacancy at various locations within the $InO_{1.5}$ and $AMO_{2.5}$ layers, Fig. 1(a), we predict the distribution of oxygen defects within the layered structure of the $InAMO_4$ compounds. We find that the location preference of the oxygen vacancy correlates with the strength of the metal-oxygen interaction, so that the vacancies are scarce in the layers formed exclusively by the light-metal oxides with strong metal-oxygen bonds, as in $InAlCaO_4$. At the same time, we show that the highly anisotropic atomic relaxation near the defect associated with the unusual fivefold oxygen coordination of the *A* and *M* atoms and the ability of Zn, Ga, and Al atoms to form stable structures with low-oxygen coordination, leads to an additional energy gain, reducing the defect formation energy below the value expected from the defect formation energies in the corresponding single-cation oxide constituents. Furthermore, the obtained insensitivity of the oxygen-vacancy formation energy to the coordination number, as found from our additional calculations of oxygen deficient ZnO phases with four-, five-, and sixfold coordinations, (i) suggests that the unusual fivefold coordination of *A* and *M* atoms in $InAMO_4$ alone cannot account for the low formation energy of oxygen vacancy in the $AMO_{2.5}$ layer and (ii) confirms that the greater freedom for atomic relaxation near the defect in the multicomponent lattice plays the decisive role in determining the defect formation.

Although the formation of other electron donor defects, e.g., cation antisite defects, must be investigated in order to determine the carrier generation mechanisms in the crystalline $InAMO_4$ compounds, the results of this paper establish general rules on the role of atomic relaxation, local oxygen coordination, and chemical composition in oxygen vacancy formation and may be instructive in understanding the properties of amorphous multicomponent semiconducting oxides where the oxygen vacancy serves as a major carrier source.[29,30]

II. APPROACH

First-principles full-potential linearized augmented plane wave method (FLAPW)[31,32] within the local density approximation is employed for the investigation of the defect formation energies and the electronic properties of $InAMO_4$ oxides (A^{3+} = Al or Ga and M^{2+} = Ca or Zn) as well as their single-cation constituents, CaO, ZnO, In_2O_3, Al_2O_3, and Ga_2O_3. Cutoffs for the basis functions, 16.0 Ry, the potential representation, 81.0 Ry, and the expansion in terms of spherical

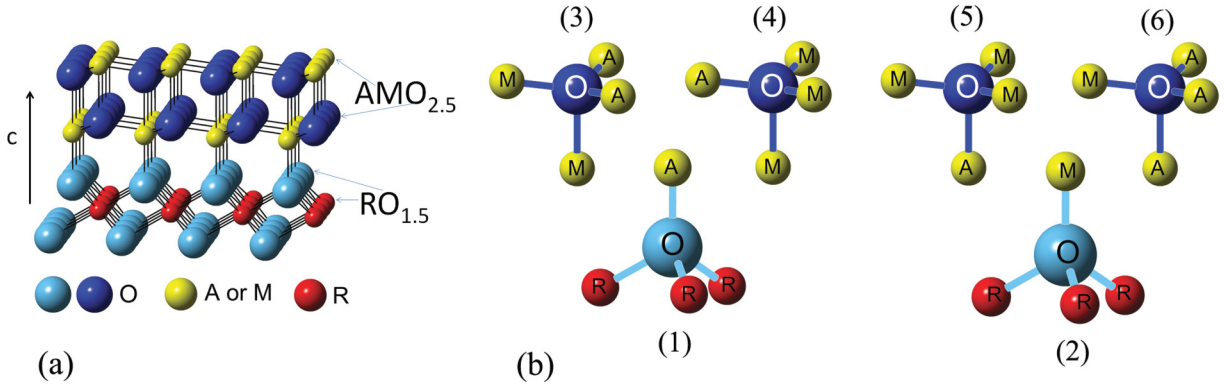

FIG. 1. (Color online) (a) Crystal structure of InAMO_4, specifically, one of the three similar blocks that construct the conventional unit cell when stacked along the z direction, is shown. (b) Six structurally different possible sites for the oxygen vacancy defect with different nearest-neighboring atoms in the layered multicomponent InAMO_4 oxides.

harmonics with $\ell \leqslant 8$ inside the muffin-tin spheres were used. The muffin-tin radii of multicomponent and single-cation oxides are as follows: 2.3 to 2.6 a.u. for In and Ca; 1.7 to 2.1 a.u. for Ga, Zn, and Al; and 1.45 to 1.8 a.u. for O atoms. Summations over the Brillouin zone were carried out using at least 23 special **k** points in the irreducible wedge.

The investigated InAMO_4 oxides have rhombohedral $R\bar{3}m$ layered crystal structure of $YbFe_2O_4$ type, Fig. 1(a).[33–36] In these compounds, In^{3+} ions have octahedral coordination with the oxygen atoms and reside in 3(a) position (Yb), whereas both A^{3+} (Al or Ga) and M^{2+} (Ca or Zn) ions reside in 6(c) position (Fe), Fig. 1, and are distributed randomly.[37] Because of the different ionic radii and the valence state of the cations in the $AMO_{2.5}$ double layer, the A^{3+} and M^{2+} atoms have different z component of the internal site position 6(c). The optimized structural parameters for every structure under consideration can be found in our previous work.[28]

To model isolated point defects in the InAMO_4 compounds, a 49-atom supercell was used with the lattice vectors $(30\bar{2})$, $(\bar{1}12)$, and $(02\bar{1})$, given in the units of the rhombohedral primitive cell vectors.[18] Note that the conventional rhombohedral unit cell of $YbFe_2O_4$ contains 21 atoms ($Z = 3$), and the primitive, i.e., the smallest volume, cell contains seven atoms ($Z = 1$). For the binary basis oxides, the following supercells were constructed; a 80-atom supercell for bixbyite In_2O_3 and corundum Al_2O_3, a 120-atom supercell for monoclinic β-Ga_2O_3, a 84-atom supercell for wurtzite ZnO, and a 128-atom supercell for rocksalt CaO. These supercells result in similar defect concentrations, namely, 1.6–1.8 $\times$ 10^{21} cm^{-3}, and, hence, similar distances between the oxygen defects $\sim$10 Å.

In our defect calculations, in addition to the band-gap correction via the screened-exchanged LDA method,[38–41] we also address the band-edge and the finite-size supercell errors in the defect calculations. We employ the correction methods proposed by Lany and Zunger,[42] namely, (i) shifting of shallow levels with the corresponding band edges of the host; (ii) band-filling correction; (iii) potential-alignment correction for supercells with charged defects; and (iv) image charge correction for charged defects via simplified Makov-Payne scheme.[42]

As mentioned above, the layered crystal structure of InAMO_4 oxides has two chemically and structurally distinct layers, $AMO_{2.5}$ and $InO_{1.5}$, which alternate along the [0001] direction. Depending on the layer and the different nearest-neighbor cations, there are several structurally different sites for the oxygen vacancy defect. Figure 1(b) shows the six possible defect sites considered for the InAMO_4 oxides. During the discussions that follow, we identify the defect sites by their nearest-neighbor atoms, specifically, by their planar and apical cations. For example, as one can see from Fig. 1(b), the sites 4 and 5 both have three neighbors of atom type M (Zn or Ca) and one neighbor of type A (Ga or Al). However, the sites are different due to the different set of the planar atoms versus the apical atom resulting in a different total energies for these sites, as it will be shown below.

The formation energy of the oxygen vacancy in three charge states, i.e., neutral V_O^0 and ionized V_O^+ or V_O^{2+}, modeled using a corresponding background charge, can be calculated as a function of the Fermi level and the corresponding chemical potential:

$$\Delta H(E_F,\mu) = E_{\text{defect}} - E_{\text{host}} + \mu_O + q(E_F), \qquad (1)$$

where E_{defect} and E_{host} are the total energies for the oxygen deficient oxide and the stoichiometric oxide in the same-size supercell, respectively; μ is the chemical potential for an oxygen atom removed from the lattice; q is the defect charge state; and E_F is the Fermi energy taken with respect to the top of the valence band.

The chemical potential $\mu_O = \mu_O^0 + \Delta\mu_O$ is taken with respect to the chemical potential μ^0 of the O_2 molecule, whereas $\Delta\mu_O$ is the deviation from the elemental chemical potential. In this work, with the purpose of reasonable comparison between the quaternary and binary oxides, we consider two extreme cases of the growth conditions. In the extreme oxygen-rich conditions, $\Delta\mu_O = 0$. In the oxygen-poor, i.e., metal-rich conditions, $\Delta\mu_O$ depends on the respective values of the heat of formation, ΔH_f(InAMO), as well as on $\Delta\mu_{\text{In}}$, $\Delta\mu_A$, and $\Delta\mu_M$ that are calculated from the following thermodynamic stability conditions. (1) In order to maintain a stable InAMO_4 host, the elemental chemical potentials should have the values

TABLE I. Calculated and experimental[45,46] heat of formation of binary oxides, ΔH_f per oxygen in electron volts, and the calculated formation energy of a neutral oxygen vacancy, $\Delta H(V_O^0)$, in electron volts, for both oxygen-poor and oxygen-rich conditions.

	ΔH_f per oxygen		$\Delta H(V_O^0)$	
	Calc	Exp	O poor	O rich
CaO	−6.00	−6.57	0.87	7.02
Al_2O_3	−4.64	−5.78	1.82	7.10
Ga_2O_3	−2.74	−3.73	0.69	3.92
ZnO	−3.42	−3.60	0.69	4.10
In_2O_3	−2.72	−3.21	1.10	3.82

that require

$$\Delta\mu_{\rm In} + \Delta\mu_A + \Delta\mu_M + 4\Delta\mu_{\rm O} = \Delta H_f({\rm In}AMO_4). \quad (2)$$

(2) To avoid the precipitation of the elements In, A, M, and O, the following conditions must be satisfied:

$$\Delta\mu_{\rm In} \leqslant 0, \quad \Delta\mu_A \leqslant 0, \quad \Delta\mu_M \leqslant 0, \quad \Delta\mu_{\rm O} \leqslant 0. \quad (3)$$

(3) To avoid the formation of the binary compounds, such as In_2O_3, A_2O_3, or MO, the following conditions must be fulfilled:

$$2\Delta\mu_{\rm O} + 3\Delta\mu_{\rm O} \leqslant \Delta H_f(In_2O_3), \quad (4)$$

$$2\Delta\mu_A + 3\Delta\mu_{\rm O} \leqslant \Delta H_f(A_2O_3), \quad (5)$$

$$\Delta\mu_M + \Delta\mu_{\rm O} \leqslant \Delta H_f(MO). \quad (6)$$

Thus the available range for the elemental chemical potentials in the case of quaternary $InAMO_4$ materials is a three-dimensional volume determined by the above stability conditions [see Eqs. (3)–(6)], projected onto the corresponding $InAMO_4$ plot [see Eq. (2)].

The heat of formation ΔH_f for the oxides is calculated with respect to the bulk orthorhombic Ga, tetragonal In, hexagonal Zn, and cubic Al or Ca. Our obtained ΔH_f values for the three representative $InGaZnO_4$, $InAlZnO_4$, and $InAlCaO_4$ compounds are –11.28 eV, –14.60 eV, and –15.40 eV, respectively. Calculating the corresponding heat of formation for the binary constituents (c.f., Table I), we find that

$$2\Delta H_f(InGaZnO_4) > \Delta H_f(In_2O_3) + \Delta H_f(Ga_2O_3) + 2\Delta H_f(ZnO), \quad (7)$$

$$2\Delta H_f(InAlCaO_4) > \Delta H_f(In_2O_3) + \Delta H_f(Al_2O_3) + 2\Delta H_f(CaO), \quad (8)$$

$$2\Delta H_f(InAlZnO_4) < \Delta H_f(In_2O_3) + \Delta H_f(Al_2O_3) + 2\Delta H_f(ZnO). \quad (9)$$

Equations (7) and (8) suggest that at zero temperature, the formation of $InGaZnO_4$ or $InAlCaO_4$ is impossible without the formation of the corresponding binary phases. This also means that there is no available elemental chemical potentials which would allow the formation of the corresponding multicomponent oxides. Since the latter are stable above 1000 °C,[33,34,36] the entropy term $T\Delta S$ must be taken into consideration. Similar arguments were reported for $In_2O_3(ZnO)_k$ compounds.[43] The entropy term can be estimated based on the corresponding equilibrium solid state reactions that involve the binary constituents as follows:

$$\Delta H_f(InGaZnO_4) - 1/2[\Delta H_f(In_2O_3) + \Delta H_f(Ga_2O_3) + 2\Delta H_f(ZnO)] = T_{InGaZnO_4} \times \delta S_{InGaZnO_4}, \quad (10)$$

$$\Delta H_f(InAlCaO_4) - 1/2[\Delta H_f(In_2O_3) + \Delta H_f(Al_2O_3) + 2\Delta H_f(CaO)] = T_{InAlCaO_4} \times \delta S_{InAlCaO_4}. \quad (11)$$

We then replace the ΔH_f for $InGaZnO_4$ and $InAlCaO_4$ with the corresponding $(\Delta H_f - T \times \delta S)$, in Eq. (2) above. As a result, the available chemical potentials for metals in $InGaZnO_4$, $InAlZnO_4$, and $InAlCaO_4$, plotted in Fig. 2, correspond to a very narrow range along the crossing line of the three planes, Eqs. (4)–(6). This is in accord with the results for Ga-free layered multicomponent $In_2O_3(ZnO)_3$ that was shown to exist without the occurrence of the secondary phases only for a constant ratio between indium and zinc.[43] For the extreme metal-rich conditions, we obtain (a) $InGaZnO_4$: $\Delta\mu_{\rm In} = \Delta\mu_{\rm Ga} = 0$, $\Delta\mu_{\rm Zn} = -0.70$ eV;

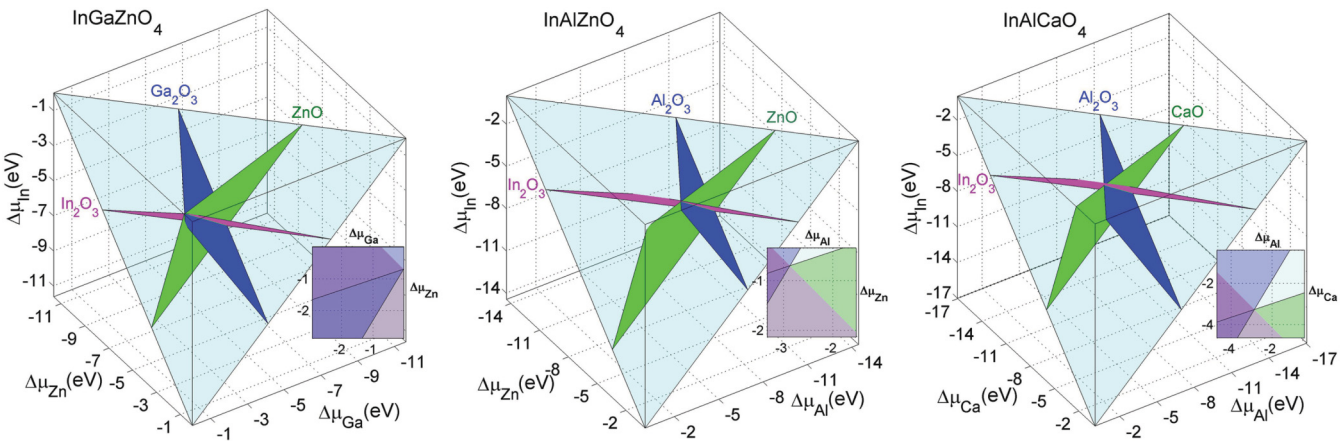

FIG. 2. (Color online) Available elemental chemical potentials for $InGaZnO_4$, $InAlZnO_4$, and $InAlCaO_4$. Shaded planes represent the stability of binary phases. The inserts show the extreme metal-rich values ($\Delta\mu_{\rm In} = 0$).

(b) $InAlZnO_4$: $\Delta\mu_{In} = 0$, $\Delta\mu_{Zn} = -0.61$ eV, $\Delta\mu_{Al} = -2.75$ eV; and (c) $InAlCaO_4$: $\Delta\mu_{In} = 0$, $\Delta\mu_{Al} = -2.9$ eV, $\Delta\mu_{Ca} = -3.3$ eV.

We stress again that for the clarity of this paper and with the purpose of fair comparison between the oxides, we do not consider intermediate oxygen pressures, i.e., when $1/4[\Delta H_f(InAMO_4) - \sum \Delta\mu_{metal}^{M\ rich}] < \Delta\mu_O < 0$. For each particular compound, the available pressure ranges are determined by the experimental characteristics, e.g., the annealing temperature, which also affects the value of $\Delta\mu_O$, as well as by the formation of other intrinsic defects. Investigations of donor and acceptor defects and, hence, possible charge compensation mechanisms (e.g., via the formation of metal vacancies which are necessary to explain the insulating behavior in the light-metal oxides) are beyond the scope of this work, and will be presented elsewhere.[44]

III. RESULTS AND DISCUSSION

A. Oxygen vacancy in binary oxides

The first step to understand the effect of the chemical composition on the formation and distribution of an oxygen vacancy in layered multicomponent $InAMO_4$ oxides, is to compare the formation energies of the oxygen defect in the corresponding binary oxides. Our calculated formation energies of the neutral oxygen defect, V_O^0, are shown in Table I, for both the extreme oxygen-poor and oxygen-rich conditions. It can be seen that the difference in the defect formation energies for the post-transition and the light-metal oxides is about 3 eV or higher in the oxygen-rich conditions ($\Delta\mu_O = 0$). The trend in the defect formation energies correlates with the heat of formation of the binary oxides, Table I: the low heat of formation of post-transition metal oxides signifies that the oxygen vacancies are abundant in these oxides. As expected, the differences in the defect formation energies become less obvious under the *extreme* metal-rich conditions, i.e., when $\Delta\mu_{metal} = 0$ and $\Delta\mu_O$ is determined by ΔH_f^{calc} according to Eqs. (4)–(6). As mentioned in the previous section, for each compound, the available pressure ranges are limited by the specific growth conditions and the formation of other intrinsic defects, which will be discussed elsewhere.[44]

Our calculated formation energies of the neutral oxygen defect V_O^0, Table I, are in a good agreement with prior reported formation energies for neutral oxygen defect in the binary oxides, such as 0.6 eV for O poor and 6.6 eV for O rich in CaO, 7.5 eV for O rich in Al_2O_3, 1.2 eV for O poor and 3.8 eV for O rich in ZnO, 1.0 eV for O poor and 3.7 eV for O rich conditions in In_2O_3.[47–50]

The fact that it is easier to create an oxygen vacancy in the post-transition metal oxides, i.e., In_2O_3 or ZnO, as compared to the light main-group metal oxides, i.e., Al_2O_3 or CaO, is in accord with the calculated degree of the electron localization around the oxygen defect.[51] A more uniform charge distribution at the bottom of the conduction band was found in the oxygen deficient post-transition metal oxides. In contrast, the light-metal oxides exhibit a strong charge confinement near the oxygen vacancy (an F-like center). It has been shown that the electron localization in the latter oxides is associated with the formation of the strong directional metal p – oxygen p bonds around the defect.[23]

We note here that Ga_2O_3 should be placed at the far end of the conventional TCO hosts such as In_2O_3 and ZnO which have low formation energy of the oxygen vacancy. In Ga_2O_3, there are three nonequivalent oxygen sites, which we label as site 1, site 2, or site 3, with three, four, or six Ga neighbor atoms at the average distance of 1.90 Å, 2.00 Å, or 1.87 Å, respectively. Consequently, the formation energies of the oxygen vacancy in those sites are different and correlate with the average Ga-O distances for each site: we obtained 1.09 eV, 1.31 eV, or 0.69 eV under the metal-rich conditions, and 4.32 eV, 4.55 eV, or 3.92 eV under the oxygen-rich conditions, for the site 1, site 2, or site 3, respectively. Note that only the lowest values are given in Table I. Since the concentration of a defect is proportional to the number of the sites available for the defect, only a third of the oxygen atoms in Ga_2O_3 may produce a vacancy defect with the formation energy similar to that in ZnO, i.e., 0.69 eV under the O-poor conditions, Table I. The higher formation energy of the V_O at the other oxygen sites (i.e., site 1 and site 2) sets Ga_2O_3 somewhat in between the two oxide groups considered above. Again, this finding is consistent with the obtained degree of the electron localization near the oxygen vacancy defect, $In_2O_3 < ZnO < Ga_2O_3 < CaO < Al_2O_3$.[51]

In this section, we also address the fundamental question about the role of the local coordination on the oxygen vacancy formation. As mentioned in Introduction, both A and M atoms in $InAMO_4$ have an unusual fivefold oxygen coordination. It has been shown[28] that this unusual coordination plays a critical role in determining the electronic properties of layered multicomponent oxides such as the band gap, the electron effective mass, and the orbital composition of the conduction band. To understand how the local coordination affects the formation energy of the oxygen vacancy, we performed defect calculations for several unstable ZnO phases, namely, for zinc blende (fourfold coordination), hypothetical wurtzite-based (fivefold), and rocksalt (sixfold) structures–in addition to the ground state wurtzite ZnO phase. For the hypothetical ZnO phase with fivefold oxygen coordination, the lattice parameters as well as the internal atomic positions were chosen so that the metal-oxygen distances are similar to the Zn-O distances in the multicomponent $InGaZnO_4$ oxide.[28] Using 84-atom supercells for wurtzite and hypothetical wurtzite-based structures and 128-atom supercells for zincblende and rocksalt structures of ZnO, we calculate the formation energy of an oxygen vacancy in these ZnO phases. We find that the defect formation energy varies insignificantly with the coordination number: it is 4.03 eV, 3.97 eV, and 4.20 eV for the zincblende (fourfold coordination), hypothetical wurtzite-based (fivefold), and rocksalt (sixfold) structures of ZnO under the extreme oxygen-rich conditions. These values are close to the defect formation energy obtained for the ground-state wurtzite ZnO phase, 4.10 eV, Table I. These results will be further discussed in Sec. III E below.

B. Distribution of oxygen vacancies in $InAMO_4$

The oxygen vacancy formation in $InGaZnO_4$ and the defect state location with respect to the conduction band edge of the oxide have been determined earlier.[23,52] In this work, we investigate how the presence of light-metal cations (Ca and/or

TABLE II. Formation energies of neutral oxygen vacancy located at six different defect sites in $InGaZnO_4$, $InAlZnO_4$, and $InAlCaO_4$ for oxygen-poor and oxygen-rich conditions. NN denotes the nearest-neighbor atoms and "a" stands for an apical atom. The lowest formation energy values are given in bold. Upon the atomic relaxation caused by the oxygen defect, the change in the distance between the vacancy and its nearest apical metal atom, ΔD-a, and the average change in the distances between the vacancy and the planar A or M atoms, ΔD^A or ΔD^M, in percent, are given.

		$InGaZnO_4$					$InAlZnO_4$					$InAlCaO_4$				
Site	NNs	O^{poor}	O^{rich}	ΔD-a	ΔD^A	ΔD^M	O^{poor}	O^{rich}	ΔD-a	ΔD^A	ΔD^M	O^{poor}	O^{rich}	ΔD-a	ΔD^A	ΔD^M
1	3R, 1A-a	1.51	4.24	+10			1.43	4.24	+16			**1.27**	**3.98**	+14		
2	3R, 1M-a	**1.32**	**4.05**	+8			**1.34**	**4.15**	+9			1.39	4.10	0		
3	2A, 2M-a	1.61	4.34	+3	–5	0	2.95	5.76	+1	+3	–1	3.26	5.97	+3	–3	–1
4	1A, 3M-a	1.38	4.12	+5	–5	–3	2.00	4.81	+3	+6	–4	2.97	5.68	+3	–1	–1
5	1A-a, 3M	1.35	4.09	+9		–8	1.57	4.38	+13		–7	2.67	5.38	+14		–1
6	3A-a, 1M	1.68	4.42	+6	–6	+1	3.14	5.95	+3	+1	–1	3.08	5.79	+1	–4	–1

Al) affects the distribution of the oxygen vacancies within the structurally and chemically distinct layers of multicomponent oxides. The chosen three $InAMO_4$ compounds, namely, $InGaZnO_4$, $InAlZnO_4$, and $InAlCaO_4$, represent the systems with none, one, and two light-metal constituents, respectively. We believe that the trends obtained for these three oxides may help us understand the role played by the composition in the defect formation and make reasonable predictions for other multicomponent oxides.

First, to determine the most energetically favorable location of the oxygen vacancy in $InGaZnO_4$, $InAlZnO_4$, and $InAlCaO_4$, we calculate the formation energies of the oxygen vacancy defect in the six structurally different oxygen sites which were discussed above and shown in Fig. 1(b). The results are given in Table II. Our comparative analysis of the defect formation energies shows that the oxygen vacancy prefers to be within the $InO_{1.5}$ layer for all three representative compounds. There are two oxygen site positions within the $InO_{1.5}$ layer, site 1 and site 2, which differ by the type of the apical atom, i.e., A or M, respectively, Fig. 1(b). Comparing the formation energies of the oxygen vacancies at these two sites, we find that in the case of $InGaZnO_4$ and $InAlZnO_4$, the oxygen vacancy defects prefer to be in the site-2 position with three In atoms and one Zn (apical) atom as their nearest neighbors. In contrast, in $InAlCaO_4$, the lowest formation energy corresponds to the defect in site 1 with three In and one apical Al as the defect nearest neighbors. We note here, that similar trends in the formation energies of the oxygen vacancy at different site positions are obtained for the ionized vacancy defect with the exception for $InGaZnO_4$ where the lowest formation energy of V_O^+ is for the defect at site 5, while the defect at site 2 is higher in energy by only 0.02 eV.

For the considered three compounds, the defect preferred site location correlates well with the experimental heat of formation of the corresponding binary oxides, and, accordingly, with the oxygen vacancy formation energy, c.f., Tables I and II. For example, in $InGaZnO_4$ or $InAlZnO_4$, In_2O_3 has the lowest heat of formation per oxygen (–3.21 eV) followed by ZnO (–3.60 eV) and Ga_2O_3 (–3.73 eV) or Al_2O_3 (–5.78 eV). Hence, the site 2 in the $InO_{1.5}$ layer corresponds to the set of the metal-oxygen bonds—three In-O bonds and one Zn-O bond—that would be easiest to break in order to create an oxygen vacancy defect. Accordingly, for the $InAlCaO_4$ oxide, the oxygen vacancy prefers to be in the site 1 with three In and one Al neighbor atoms rather than in the site 2 with three In and one Ca neighbors, since CaO has stronger metal-oxygen bonds than Al_2O_3.

The above results suggest that the oxygen vacancy has a preference to form within the $InO_{1.5}$ layer, independent of the chemical composition of the $AMO_{2.5}$ layer in the three compounds. However, the preference for the octahedral $InO_{1.5}$ layer is strong only for $InAlCaO_4$: the vacancy formation energy in the $AlCaO_{2.5}$ layer is higher by at least 1.3 eV than that for the oxygen vacancy defect in the $InO_{1.5}$ layer, Table II. In marked contrast to $InAlCaO_4$ with two light-metal constituents, the oxygen vacancy distribution is likely to be more uniform throughout the layered structure of $InGaZnO_4$ and $InAlZnO_4$. In $InGaZnO_4$, the difference in the defect formation energies between site 2 (three In and one Zn) and sites 4 and 5 (three Zn and one Ga) is negligible, 0.03 eV. Therefore one can expect the vacancy concentrations to be comparable in the $InO_{1.5}$ and $GaZnO_{2.5}$ layers of $InGaZnO_4$. In $InAlZnO_4$, the difference in the defect formation energies between site 2 and site 5 is larger, about 0.2 eV. In this case, we can estimate that the resulting defect concentrations will differ by about an order of magnitude at 1000 K (which is a typical annealing temperature in these oxides). Figure 3 shows the estimated concentrations of the oxygen vacancy defect in the neutral charge state in the $InO_{1.5}$ and $AMO_{2.5}$ layers as a function of growth temperature. The figure clearly illustrates that the presence of one light-metal constituent in the mixed $AMO_{2.5}$ layer reduces the concentration of the electron donor defect in that layer, but does not suppress it completely as in the case when both A and M atoms are light metals. We note that other charge states of the oxygen vacancy may contribute to the overall V_O concentration if acceptor defects such as cation vacancies, oxygen interstitials, and/or antisite defects, become abundant pushing the equilibrium Fermi level away from the conduction band.

Finally, the uniform distribution of the oxygen defect throughout the layered structure of $InGaZnO_4$ contradicts the observed anisotropy of the electrical properties in this material.[53] Indeed, it is unlikely that oxygen vacancy is a major electron donor in equilibrium-grown $InGaZnO_4$ since the defect is a deep donor.[23]

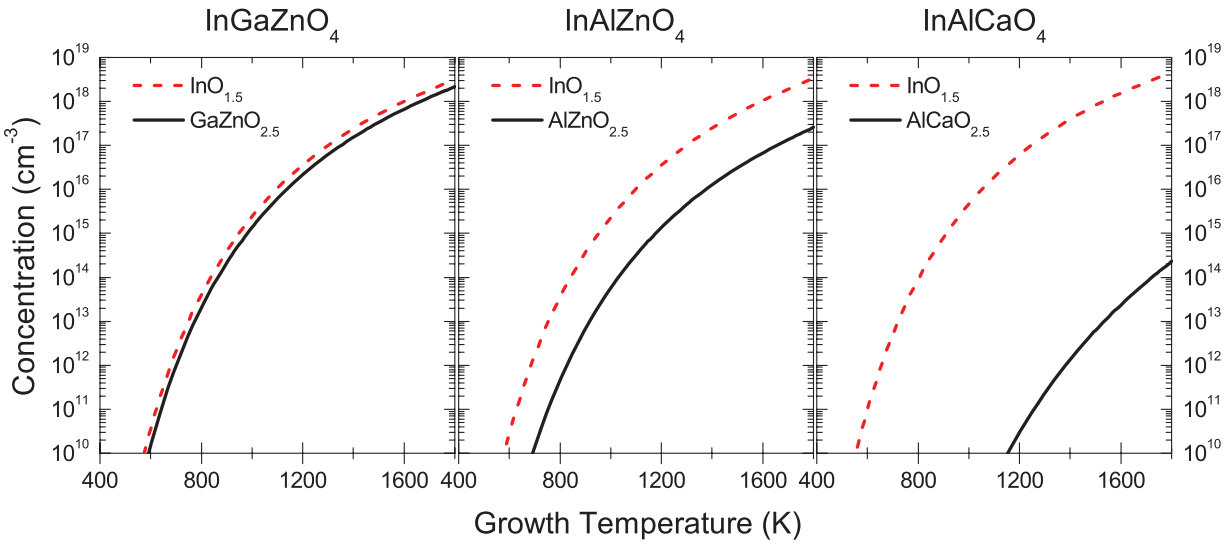

FIG. 3. (Color online) Concentrations of the oxygen vacancy defect in the *neutral* charge state in the $InO_{1.5}$ and $AMO_{2.5}$ layers as a function of growth temperature calculated under the extreme oxygen-poor conditions.

C. Formation of stable fourfold structures in oxygen deficient InAMO_4

Comparing the energetics for the six different defect sites, we find another trend that can be explained based on the heat of formation of the constituent binary oxides. Specifically, in $InAlZnO_4$, the defect formation energy, $\Delta H(V_O)$, increases as the number of the Al atoms around the oxygen defect increases: site 1 (one apical Al and three In) < site 5 (one apical Al and three Zn) < site 4 (one planar Al) < site 3 (two planar Al) < site 6 (two planar and one apical Al). Therefore the oxygen vacancy in $InAlZnO_4$ "avoids" having Al as a neighbor cation. Indeed, the Al-O bond is the strongest compared to the In-O and Zn-O bonds in $InAlZnO_4$, and the oxygen vacancy defect is least likely to be formed near the Al atoms. This tendency is stronger when the Al is a planar neighbor rather than the apical one simply because the planar metal-oxygen distances are generally shorter than the apical ones in the layered InAMO_4 compounds.[28]

Similar to $InAlZnO_4$, the oxygen vacancy distribution exhibits a trend with respect to Ga in $InGaZnO_4$, where the formation energy of the defect in the sites with one Ga neighbor (sites 1, 4, and 5) is lower than that in the site 3 (two Ga neighbors) or site 6 (three Ga neighbors). However, simple arguments based on the comparison of the heat of formation of the binary oxides do not explain all the results obtained. In particular, in $InGaZnO_4$ the formation energy of the oxygen vacancy at site 5 (three Zn and one Ga neighbor) is lower than the one at site 1 (three In and one Ga) although the heat of formation of In_2O_3 is lower as compared to that of ZnO, Table I. We believe that one of the possible explanations involves the cation preference for a particular oxygen coordination. For instance, in the ground-state phase of ZnO, the wurtzite structure, Zn is in fourfold coordination with O atoms. In bixbyite In_2O_3 as well as in other available phases for indium oxide, In is always sixfold coordinated with O atoms. In $InGaZnO_4$ compound, all Zn (and Ga) atoms are in fivefold coordination with oxygen atoms whereas In atoms remain in the sixfold coordination. After removal of the oxygen atom in site 5, three Zn atoms become fourfold coordinated with oxygen. Owing to the preference of Zn atoms to be in the fourfold coordination, the defect in site 5 (or site 4) become energetically more favorable compared to the site-1 defect where three In atoms lose one oxygen neighbor and become fivefold coordinated. (As it will be shown in the next section below, Zn atoms near the defect experience much stronger relaxation, with the Zn-V_O^0 distances reduced by 8 % for the site-5 case, Table II, whereas the In-V_O^0 distances change only by 1–2 %.)

Accordingly, the most stable configuration of the oxygen defect in the $AlZnO_{2.5}$ layer of $InAlZnO_4$ corresponds to the structure with three fourfold coordinated Zn (site 5). The formation energy in this case is higher by only 0.14 eV as compared to the defect at site 1, Table II. (As it will be discussed below, Zn relaxation is restricted due to the presence of the strong Al-O bonds that limits the ability of Zn to form a more stable fourfold coordinated structure.)

In marked contrast to Zn, Ca does not exhibit a preference for fourfold coordination being sixfold-coordinated with oxygen in the ground state (rocksalt structure) as well as in most CaO-Al_2O_3 structures.[54] Thus, in $InAlCaO_4$, the difference between the formation energies in site 1 and site 5 is large, 1.4 eV, and is mainly determined by the differences in the metal-oxygen interaction in the corresponding binary oxides, Table I. In other words, there is no additional energy gain associated with the formation of a stable fourfold structure similar to the one observed in the case of Zn, since Ca is indifferent to the formation of such structure and, as it will be shown below, experience negligible relaxation upon oxygen removal—in marked contrast to Zn in $InGaZnO_4$ and $InAlZnO_4$.

While Zn shows a strong preference for the fourfold coordination, Al and Ga can exist in either sixfold or fourfold oxygen coordination. The corundum Al_2O_3 has octahedrally coordinated Al atoms, but there are many stable oxide phases where Al is in fourfold coordination with oxygen.[54] Ga_2O_3 has two nonequivalent Ga atoms in the ground-state monoclinic

phase: one being fourfold coordinated and the other in sixfold coordination. Therefore we believe that both Al and Ga can form a stable fourfold structure when losing one oxygen atom upon introduction of an oxygen vacancy in the InAMO_4 compounds. The formation of such structures is illustrated below based on the atomic relaxation near the oxygen defect.

D. Structural relaxation in oxygen deficient InAMO_4

The vacancy formation and distribution in InAMO_4 can be further understood by considering the structural relaxation caused by the defect. For this, we compared the changes in the positions of the metal and oxygen atoms near the vacancy defect. Table II shows how much the metal atoms nearest to the oxygen vacancy shift with respect to their original positions in the stoichiometric oxide. First of all, we note that in all three multicomponent oxides, the apical atoms move away from the defect (positive ΔD-a) and the values are generally larger compared to the change in the planar distances, $\Delta D^{A/M}$, some of which are positive (cations move away from the defect), while others are negative (cations get closer to the defect). The larger relaxation of the apical atoms is inherent to the layered structure of InAMO_4 compounds: stacking the cations of different ionic radius, valence, and metal-oxygen bond strength along the c direction leads to larger deviations from the regular metal-oxygen distances in the corresponding binary oxides,[28] and hence allows more freedom for relaxation.

Comparing the apical atom's shifts, ΔD-a, for $InGaZnO_4$ and $InAlCaO_4$, we find that the shifts are comparable for both Ga and Zn apical atoms in the former oxide, whereas in the two-light-metal compound, apical Al atoms exhibit more significant changes, 14%, compared to the apical Ca atoms, 0–3%. Accordingly, the Ca planar atoms exhibit only a small relaxation, $\Delta D^{\mathrm{Ca}} \sim 1$ % for all vacancy sites, as compared to the planar Zn, Al, and Ga atoms shifts. The negligible relaxation of Ca as compared to the relaxation of Zn, Al, or Ga, can be explained by several factors: (i) the large ionic radius of Ca ion as compared to those of Zn, Ga and Al (given in the order of decreasing ionic radii), (ii) the stronger bonds between Ca and its nearest O neighbors with respect to the oxygen bonds with Zn, Ga, and Al, as determined by the heat of formation of the binary oxides, Table I, and (iii) Ca indifference to losing one oxygen neighbor to become a fourfold coordinated cation. All the factors above limit the motion of Ca in the lattice with oxygen defect. In contrast to Ca atoms, the smaller ionic radius, weaker metal-oxygen bonds, and a possibility to form a fourfold structure make it easier for Al, Zn, and Ga to adjust to the new electronic environment created by the oxygen defect and, hence, those atoms experience greater relaxation (see Table II).

Further confirmation of our observations above can be obtained based on the optimized distances between the metal atoms that surround the defect and their oxygen neighbors. We find that in $InGaZnO_4$, the atomic relaxation results in slightly increased planar Zn-O distances (from ∼1.98 Å to ∼2.05 Å) and notably decreased apical Zn-O distance (from 2.41 Å to ∼2.20 Å) making all four Zn-O distances more alike to resemble the fourfold coordination. Similarly, the apical Ga atoms near the vacancy pull their oxygen neighbors to become four-coordinated with oxygen: all four Ga-O distances are found to be within 1.86–1.89 Å, which is close to the distances between the fourfold coordinated Ga and oxygen atoms in monoclinic Ga_2O_3, 1.83–1.86 Å (for comparison, the distances between the sixfold coordinated Ga and oxygen atoms in monoclinic Ga_2O_3 are 1.93–2.07 Å).

Significantly, we find that Zn propensity to become fourfold-coordinated upon losing an oxygen neighbor decreases in $InAlZnO_4$ as compared to $InGaZnO_4$, i.e., when Ga atoms in the A sublattice are changed to Al. First of all, we note that the planar Zn-O distances in $InAlZnO_4$ (2.02–2.21 Å) are larger than the corresponding Zn-O distances in $InGaZnO_4$ (1.99–2.13 Å) or the planar Zn-O distances in wurtzite ZnO (1.97 Å). This suggests that the motion of Zn atoms in oxygen deficient $InAlZnO_4$ is restricted due to the stronger Al-O bonds present in the $AlZnO_{2.5}$ layer. Indeed, we obtain that the distances between the Zn atoms nearest to the oxygen defect (in site- 5) and their oxygen apical neighbors reduce by only 0–2%, from ∼2.44 Å to ∼2.38 Å, whereas the corresponding changes of the Zn-O distances in $InGaZnO_4$ are 3–4%. Similarly, the change in the distance between the oxygen defect and the nearest apical Zn, ΔD-a, is smaller in $InAlZnO_4$ (1–3%) than in $InGaZnO_4$ (3–5%), see Table II.

Comparing the relaxation of Al atoms in $InAlZnO_4$ and $InAlCaO_4$ with the oxygen vacancy at site-1, we observe a similar tendency: in the former, the Al pulls its nearest oxygen atoms closer to itself so that all four Al-O distances become nearly identical (changing from 1.87–1.96 Å to 1.80–1.82 Å) with the largest distance change of 8%, whereas in $InAlCaO_4$, all four Al-O distances are essentially unchanged upon introduction of the defect having the largest relaxation of only 0.4%. Therefore we can conclude that the presence of the metal atoms which form stronger bonds with the oxygen neighbors restricts the motion of the metals with weaker oxygen bonds. As a result, the latter cations are unable to form a preferred coordination and/or relax to the desired metal-oxygen distances and are forced to remain in a highly anisotropic oxygen environment upon introduction of a oxygen vacancy. This leads to a high formation energy of the defect. Indeed, the formation of strong directional bonds due to significant contribution from the metal p orbitals near the oxygen vacancy defect in Al_2O_3, CaO, and MgO,[23] was shown to be the reason for the strong electron localization near the vacancy in these binary light-metal oxides. In contrast, when the multicomponent oxide consists of a low-formation oxide constituents, as in the case of $InGaZnO_4$, the weakly bonded lattice may allow for a significant atomic relaxation, hence, leading to an energy gain due to the formation of more stable structures, and thus a more uniform defect distribution throughout the lattice (c.f., Fig. 3).

E. Vacancy distribution in $InGaZnO_4$ versus $In_2O_3(ZnO)_3$

As discussed above, the formation energies of the oxygen defect in the $InO_{1.5}$ and $GaZnO_{2.5}$ layers of $InGaZnO_4$ are nearly identical, hence, a uniform vacancy distribution within the lattice is expected. These finding differs from the results obtained for $In_2O_3(ZnO)_3$ where the oxygen vacancy distribution was found to be anisotropic.[43] We believe that the difference arises from a larger variety of oxygen coordinations in $In_2O_3(ZnO)_3$ where there are six- and fivefold

coordinated In as well as five- and fourfold coordinated Zn, whereas in $InGaZnO_4$ each cation has only one oxygen coordination—sixfold In and five-fold Zn or Ga. The greater freedom for the atomic relaxation around an oxygen vacancy in $In_2O_3(ZnO)_3$ leads to an additional energy gain and, hence, lower defect formation energy in this material. Indeed, in the Ga-free compound, the formation energies of the neutral oxygen vacancy varies over a wide range, from 0.2 eV to 1.4 eV, depending on the nearest-neighbor cations and their coordination. Our formation energies for the oxygen defect in the neutral charge state in $InGaZnO_4$ are within a notably narrower range, from 1.6 eV to 1.9 eV calculated at the same growth conditions, $T = 1573$ K and $pO_2 = 0.0001$ atm. In the Sec. III A above, we showed that the formation energy of the oxygen defect varies insignificantly with the coordination number in several ZnO phases. This finding, along with the fact that the lowest formation energies of the neutral oxygen defect in $In_2O_3(ZnO)_3$ are significantly lower (by as much as $\sim$1 eV) as compared to those in binary In_2O_3 and ZnO,[49] supports our conclusion on the important role of atomic relaxation in the defect formation in multicomponent oxides.

Comparing $InGaZnO_4$ and $In_2O_3(ZnO)_3$, there is only one defect site location with similar nearest neighbor cations, namely three sixfold In atoms and one fivefold Zn atom, in the oxides. The formation energies of the neutral oxygen vacancy in this site are found to be close, namely, 1.6 eV in $InGaZnO_4$ and 1.2 eV in $In_2O_3(ZnO)_3$ for the same growth conditions of $T = 1573$ K and $pO_2 = 0.0001$ atm. The difference may be attributed to the different metal-oxygen distances as well as to a stronger atomic relaxation in $In_2O_3(ZnO)_3$, as discussed above.

IV. CONCLUSIONS

We have investigated the oxygen vacancy formation in three representative multicomponent $InAMO_4$ compounds with none, one, and two light metal constituents. We find that the oxygen defect prefers to be located in the $InO_{1.5}$ layer for all three $InAMO_4$ materials, which correlates well with the fact that In_2O_3 has the lowest heat of formation among the corresponding binary oxides. However, the formation energy for the oxygen vacancy located in the $AMO_{2.5}$ layer is higher by only 0.03 eV in $InGaZnO_4$ and by 0.23 eV in $InAlZnO_4$ as compared to the defect in the $InO_{1.5}$ layer of the corresponding oxide. We show that for the oxygen vacancy in the $AMO_{2.5}$ layer, the additional energy gain is due to a large atomic relaxation near the defect and the formation of stable fourfold structures for Zn, Al, and Ga atoms. The comparable formation energies for the defects in the two structurally distinct layers result in a more uniform distribution of the oxygen defect throughout the layered structure of $InGaZnO_4$ and $InAlZnO_4$.

Although investigations of other electron donor defects (cation antisites) as well as acceptor defects (cation vacancies) are necessary in order to determine the carrier generation mechanism in the $InAMO_4$ compounds, the results of this work allow us to derive general rules about the role of chemical composition, local oxygen coordination, and atomic relaxation in the formation of oxygen vacancies. Specifically, we establish that the formation energy of the oxygen vacancy depends not only on the strength of the metal-oxygen bonds, as expected from the oxide heat of formation,[46] but also on (i) the ability of the defect's neighbor cations to form stable structures with low oxygen coordination and (ii) the ability of the multicomponent lattice to adjust to a new environment created by the defect by allowing for a substantial atomic relaxation.

The above rules are instructive in search for alternative light-metal oxide constituents. In particular, we propose germanium oxide[55] as a promising candidate for the following two reasons. First, the relatively low heat of formation of GeO_2, namely, $\Delta H_f = -5.59$ eV (which is similar to the heat of formation of SnO_2, $\Delta H_f = -6.02$ eV, a widely used constituent of multicomponent transparent conductive oxides) is expected to allow for an appreciable atomic relaxation in the lattice in order to achieve the desired local structure characteristics (i.e., metal-oxygen distances and coordination) for all constituents and, hence, reduce the multicomponent lattice strain. The second appealing characteristic of GeO_2 is that the Ge cations can exist in both fourfold and sixfold coordination, therefore, they are likely to adjust to anisotropic oxygen environment associated with the formation of oxygen defects, hence, reducing the donor defect formation energy.

ACKNOWLEDGMENTS

This work was supported by the NSF Grants No. DMR-0705626 and DMR-1121262. Computational resources are provided by the NSF-supported XSEDE.

*juliaem@mst.edu

[1] K. L. Chopra, S. Major, and D. K. Pandya, Thin Solid Films **102**, 1 (1983).
[2] A. L. Dawar and J. C. Joshi, J. Mater. Sci. **19**, 1 (1984).
[3] D. S. Ginley and C. Bright, MRS Bull. **25**, 15 (2000).
[4] R. Gordon, MRS Bull. **25**, 52 (2000).
[5] A. J. Freeman, K. R. Poeppelmeier, T. O. Mason, R. P. Chang, and T. J. Marks, MRS Bull. **25**, 45 (2000).
[6] T. Minami, MRS Bull. **25**, 38 (2000).
[7] P. P. Edwards, A. Porch, M. O. Jones, D. V. Morgan, and R. M. Perks, Dalton Trans. **19**, 2995 (2004).
[8] H. Kawazoe and K. Ueda, J. Amer. Ceram. Soc. **82**, 3330 (1999).
[9] T. Moriga, D. R. Kammler, T. O. Mason, G. B. Palmer, and K. R. Poeppelmeier, J. Am. Ceram. Soc. **82**, 2705 (1999).
[10] H. Mizoguchi and P. M. Woodward, Chem. Mater. **16**, 5233 (2004).
[11] G. J. Exarhos and X.-D. Zhou, Thin Solid Films **515**, 7025 (2007).
[12] E. Fortunato, D. Ginley, H. Hosono, and D. C. Paine, MRS Bull. **32**, 242 (2007).
[13] B. J. Ingram, G. B. Gonzalez, D. R. Kammler, M. I. Bertoni, and T. O. Mason, J. Electroceram. **13**, 167 (2004).
[14] H. Hosono, J. Non-Cryst. Solids **352**, 851 (2006).

[15] A. Facchetti and T. Marks, *Transparent Electronics: From Synthesis to Applications* (Wiley, New York, 2010).
[16] D. S. Ginley, H. Hosono, and D. C. Paine, *Handbook of Transparent Conductors* (Springer, Berlin, 2011).
[17] J. E. Medvedeva, A. J. Freeman, M. I. Bertoni, and T. O. Mason, Phys. Rev. Lett. **93**, 016408 (2004).
[18] J. E. Medvedeva, Europhys. Lett. **78**, 57004 (2007).
[19] J. E. Medvedeva, Appl. Phys. A **89**, 43 (2007).
[20] M. Bertoni, T. Mason, J. Medvedeva, A. Freeman, K. Poeppelmeier, and B. Delley, J. Appl. Phys. **97**, 103713 (2005).
[21] M. Bertoni, J. Medvedeva, Y. Q. Wang, A. Freeman, K. R. Poeppelmeier, and T. Mason, J. Appl. Phys. **102**, 113704 (2007).
[22] S. Jin *et al*., Chem. Mater. **20**, 220 (2008).
[23] J. E. Medvedeva and C. L. Hettiarachchi, Phys. Rev. B **81**, 125116 (2010).
[24] A. Walsh, J. D. Silva, and S. Wei, J. Phys.: Condens. Matter **23**, 334210 (2011).
[25] Y. Ke, J. Berry, P. Parilla, A. Zakutayev, R. O'Hayre, and D. Ginley, Thin Solid Films **520**, 3697 (2012).
[26] C. Yang, X. Li, X. Gao, X. Cao, R. Yang, and Y. Li, Solid State Commun. **151**, 264 (2011).
[27] J. Robertson, R. Gillen, and S. Clark, Thin Solid Films **520**, 3714 (2012).
[28] A. Murat and J. E. Medvedeva, Phys. Rev. B **85**, 155101 (2012).
[29] K. Nomura, T. Kamiya, H. Ohta, T. Uruga, M. Hirano, and H. Hosono, Phys. Rev. B **75**, 035212 (2007).
[30] T. Kamiya, K. Nomura, M. Hirano, and H. Hosono, Phys. Status Solidi C **5**, 3098 (2008).
[31] E. Wimmer, H. Krakauer, M. Weinert, and A. J. Freeman, Phys. Rev. B **24**, 864 (1981).
[32] M. Weinert, E. Wimmer, and A. J. Freeman, Phys. Rev. B **26**, 4571 (1982).
[33] V. K. Kato, I. Kawada, N. Kimizuka, and T. Katsura, Z. Kristallogr. **141**, 314 (1975).
[34] N. Kimizuka and T. Mohri, J. Solid State Chem. **60**, 382 (1985).
[35] N. Kimizuka and T. Mohri, J. Solid State Chem. **78**, 98 (1989).
[36] T. M. N. Kimizuka and Y. Matsui, J. Solid State Chem. **74**, 98 (1988).
[37] C. Li, Y. Bando, M. Nakamura, and M. Kimizuka, J. Electron Microsc. **46**, 119 (1997).
[38] D. M. Bylander and L. Kleinman, Phys. Rev. B **41**, 7868 (1990).
[39] R. Asahi, W. Mannstadt, and A. J. Freeman, Phys. Rev. B **59**, 7486 (1999).
[40] C. B. Geller, W. Wolf, S. Picozzi, A. Continenza, R. Asahi, W. Mannstadt, A. J. Freeman, and E. Wimmer, Appl. Phys. Lett. **79**, 368 (2001).
[41] M. Y. Kim, R. Asahi, and A. J. Freeman, J. Comput.-Aided Mater. Des. **9**, 173 (2002).
[42] S. Lany and A. Zunger, Phys. Rev. B **78**, 235104 (2008).
[43] H. Peng, J.-H. Song, E. M. Hopper, Q. Zhu, T. O. Mason, and A. J. Freeman, Chem. Mater. **24**, 106 (2012).
[44] A. Murat and J. E. Medvedeva (unpublished).
[45] T. B. Reed, *Free Energy of Formation of Binary Compounds* (MIT Press, Cambridge, Massachusetts, 1971).
[46] *Lange's Handbook of Chemistry*, edited by J. Dean (McGraw-Hill, New York, 1999).
[47] J. Osorio-Guillén, S. Lany, S. V. Barabash, and A. Zunger, Phys. Rev. Lett. **96**, 107203 (2006).
[48] K. Matsunaga, T. Tanaka, T. Yamamoto, and Y. Ikuhara, Phys. Rev. B **68**, 085110 (2003).
[49] S. Lany and A. Zunger, Phys. Rev. Lett. **98**, 045501 (2007).
[50] I. Tanaka, K. Tatsumi, M. Nakano, and H. Adachi, J. Am. Seram. Soc. **85**, 68 (2002).
[51] J. E. Medvedeva, in *Transparent Electronics: From Synthesis to Applications* (Wiley, New York, 2010), pp. 1–29.
[52] H. Omura, H. Kumomi, K. Nomura, T. Kamiya, M. Hirano, and H. Hosono, J. Appl. Phys. **105**, 093712 (2009).
[53] H. Hiramatsu, H. Ohta, W. S. Seo, and K. J. Koumoto, J. Jpn. Soc. Powder Powder Metall. **44**, 44 (1997).
[54] J. E. Medvedeva, E. N. Teasley, and M. D. Hoffman, Phys. Rev. B **76**, 155107 (2007).
[55] H. Mizoguchi, T. Kamiya, S. Matsuishi, and H. Hosono, Nat. Commun. **2**, 470 (2011).